Transaction of the Korean Society of Mechanical Engineers, Vol. 8, No. 5, pp. 505~515, 1984. 505

<Original>

Forced Convective Heat Transfer over a Wedge in the Region of Multiple Steady States

Kap Jong Riu*, Won Ick Jang and Byung Ha Kim****

(Received May 22, 1984)

多重定常狀態區域에서 쐐기面에 의한 强制對流熱傳達

劉 甲 鍾 · 張 元 翼 · 金 炳 河

抄　錄

同一한 物理的인 因子와 境界條件下에서, 서로 다른 두 개 以上의 流動이나 熱傳達이 發生되는 多重定常狀態에 對한 現象은 最近 自然科學이나 工業分野에서 매우 重要視되어지고 있다. 그 한 예로서 $-0.1988<\beta<0$ 領域에서 쐐기面에 따른 流動現象이 多重定常狀態가 됨을 Stewartson에 依해 밝혀진 바 있다. 이 領域에서 周圍流體가 空氣($Pr=0.72$)이고, 쐐기面이 여러가지 熱流束을 가지는 境遇에 對해서 强制對流熱傳達을 multiple shooting 方法으로 理論解析하였다. 그 結果, 相異한 두 개의 熱傳達媒介變數 즉 多重解가 얻어져서 多重定常狀態의 强制對流熱傳達이 일어남을 알았다.

Nomenclature

f	: Dimensionless stream function
f'	: Dimensionless velocity
f''	: Dimensionless shear
$f''(0)$	: Flow parameter
m	: Index of main stream velocity
n	: Index of wedge surface temperature
Nu_x	: Local Nusselt number
P	: Pressure of fluid
Pr	: Prandtl number
Re	: Reynolds number
Re_x	: Local Reynolds number
T	: Local temperature of fluid
$T_0(x)$	: Temperature of wedge surface
T_∞	: Free stream temperature
$U_\infty(x)$	: Main stream velocity
u, v	: Velocity componenents in x and y directions
x, y	: Cartesian coordinates
α	: Thermal diffusivity
β	: Pressure gradient parameter
δ	: Velocity boundary-layer thickness
δ_t	: Temperature boundary-layer thickness
η	: Similarity variable
μ	: Dynamic viscosity
ν	: Kinematic viscosity

* Member, Kyungpook National University
**Graduate School, Kyungpook National University

ρ : Density of fluid

τ : Shear stress

ϕ : Dimensionless temperature

$-\left(\frac{m+1}{2}\right)^{1/2}\phi'(0)$: Heat-transfer parameter $[=Nu_x/(Re_x)^{1/2}]$

ψ : Stream functfon

1. Introduction

Laminar boundary layers exhibiting similarity have long been the subject of numerous studies since they play an important role in illustrating the main physical features of boundary layer phenomena. The problem of forced convective heat transfer over a wedge is an important one, since the wedge geometry covers several practical flow circumstances, such as the stagnation flow and the flow over inclined and vertical surfaces.

Probably the most famous similarity equation for incompressible laminar boundary layer flow is the Falkner-Skan equation[1].

Later, Hartree[2] investigated the Falkner-Skan equation in detail by step-by-step integration and iterative techniques with the Manchester differential analyzer, and obtained solutions for several values of β in the range of $-0.1988<\beta<2.4$.

Stewartson[3] presented a detailed analysis for laminar and incompressible flow over a wedge. According to this analysis, in the range of increasing pressure($-0.1988<\beta<0$), there exists a further solution, that is, in addition to the one discovered by Hartree. The additional solution leads to a velocity profile with back flow, and it has been used in aerodynamics as a basis for calculation of flows past separation. In addition, it was shown that if $-0.5<\beta<0$ there is a family of solutions corresponding to boundary layers bounded on one side by free streamlines.

Levy[4] and Imai[5] studied the heat transfer to constant-property laminar boundary layer with power-function variation of free stream velocity and of temperature difference between wall and free stream by means of numerical computations. They proposed an empirical formula for the local heat transfer coefficient in accelerated and retarded flows.

Stojanovic[6] investigated the conditions for the existence of similarity solutions to the energy equation for wedge flows, rotating bodies of revolution, and bodies of revolution in a rotating fluid.

Cebeci and Keller[7] employed a parallel shooting method for solving the Falkner-Skan equation in the region of reversed flow($-0.198851<\beta<0$).

Lees and Reeves[8] gave a physical description of the flow pattern for adiabatic boundary layer/shock-wave interaction, employing of the Stewartson family of velocity profiles.

The small separation bubbles which form near the leading edge of airfoils prior to the onset of leading-edge stall had been analyzed by Orimi and Reeves[9], including the similar solution for reversed flow found by Stewartson was employed for analyzing the free shear layer.

It has been found by many previous investigations(e.g. Saitoh[10], Zandbergan & Dijkstra [11], Lentini & Keller[12], Gebhart et al[13]) that there exist multiple steady states in convective heat transfer problems. To the best knowledge of the present authors, there is no previous study dealing with forced convective heat transfer over a wedge in the region of multiple steady states.

The purpose of the present work is to investigate the change of heat transfer parameter and the temperature distribution according to pressure gradient parameter in the wedge flow under multiple steady state conditions. Boundary conditions of wedge surface under present investigation are four particular cases, i.e. isothermal, uniform heat flux, two of variable temperature when an ambient fluid is air.

The new solutions have been computed by two methods. The first is a simple and well-known tool, that of suspending (addition below) a new differential equation $d\beta/d\eta=0$ to the system under consideration. This additional equation permits one to introduce a new boundary condition containing a parameter that can be varied as desired to generate a family of solutions to the boundary-value problem by continuation. The second method is the use of state-of-the-art two-point boundary-value problem code, a multiple shooting code, BOUNDS.

2. Analysis

The analysis of forced convective heat transfer over a wedge in the region of multiple steady states is studied under the following assumptions and conditions.

(1) The flow is two-dimensional steady laminar motion.

(2) The fluid is incompressible and all fluid properties remain constant.

(3) Only velocity gradient in the y-direction produces viscous stresses which are large enough to be taken into account.

(4) The fluid momentum in the y-direction is negligible compared with momentum in the x-direction.

(5) There are no energy dissipation and no body forces in the boundary layer.

(6) The Reynolds number is large.

The resulting laminar boundary-layer equations and boundary conditions under the above assumptions can be written as:

$$\frac{\partial u}{\partial x}+\frac{\partial v}{\partial y}=0 \tag{1}$$

$$u\frac{\partial u}{\partial x}+v\frac{\partial u}{\partial y}=\nu\frac{\partial^2 u}{\partial y^2}-\frac{1}{\rho}\frac{\partial p}{\partial x} \tag{2}$$

$$u\frac{\partial T}{\partial x}+v\frac{\partial T}{\partial y}=\alpha\frac{\partial^2 T}{\partial y^2} \tag{3}$$

$$u(x,0)=v(x,0)=0,\quad u(x,\infty)=U_\infty(x)$$
$$T(x,0)=T_0(x),\quad T(x,\infty)=T_\infty \tag{4}$$

In writing the above equations, cartesian coordinate system has been employed as shown in Fig. 1.

For similarity, the main stream velocity satisfies the following relationship[14]

$$U_\infty(x)=Ax^m,\quad m=\frac{\beta}{2-\beta} \tag{5}$$

where A and β are constants. Clearly A is the value of velocity at the point where x is of unit length and the value of β depends on the pressure gradient in the stream direction. Although β is constant for any given similar boundary layer, by taking a range of different values it serves as the pressure gradient parameter. There is marked difference in the behavior of boundary layer fluid in the ranges of decreasing and increasing pressure, respectively.

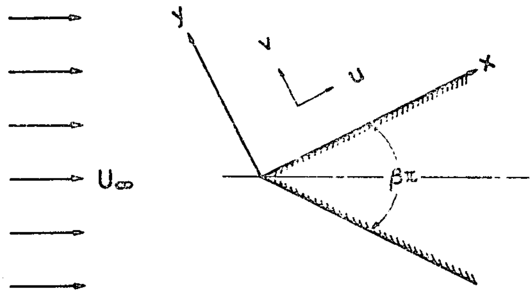

Fig. 1 Coordinate system

Following the notation of Gebhart[15], we define a transformation in terms of a similarity variable η and a stream function f and also define the temperature function ϕ

$$\eta=yb(x),\ \psi=\nu c(x)f(\eta),\ \phi=\theta(x,y)/d(x)$$
$$\theta(x,y)=T(x,y)-T_\infty,\ b(x)$$

$$=\frac{1}{x}\left(\frac{m+1}{2}Re_x\right)^{1/2} \quad (6)$$

$$c(x)=\left(\frac{2}{m+1}Re_x\right)^{1/2},$$

$$d(x)=T_0(x)-T_\infty=Nx^n$$

where N is the value of temperature at the point where x is of unit langth, and the stream function ψ is defined as

$$u=\frac{\partial\psi}{\partial y},\ v=-\frac{\partial\psi}{\partial x}. \quad (7)$$

When the conditions for similarity are satisfied, the set of partial differential equations (1) through(3) can be transformed to a much simpler group of ordinary differential equations in terms of the similarity variables(6) as follows:

$$f'''+ff''+\beta(1-f'^2)=0 \quad (8)$$

$$\phi''+Prf\phi'-\frac{2nPr}{m+1}f'\phi=0 \quad (9)$$

With similarity, the apparent boundary conditions are given as follows:

$$f(0)=f'(0)=f'(\infty)-1=\phi(0)-1$$
$$=\phi(\infty)=0 \quad (10)$$

where primes denote differentiation with respect to η. Then, the flow parameter (11) and the heat transfer parameter (12) can be obtained as follows:

$$\tau/\frac{\mu U_\infty(x)}{x}\cdot(Re_x)^{1/2}=f''(0) \quad (11)$$

$$\frac{Nu_x}{(Re_x)^{1/2}}=-\left(\frac{m+1}{2}\right)^{1/2}\cdot\phi'(0) \quad (12)$$

The present analysis considered for the following four particular wedge surface conditions.

Case 1 : An isothermal wedge surface($n=0$).

Case 2 : A wedge surface with uniform heat flux$\left(n=\frac{1-m}{2}, m\neq 1\right)$.

Case 3 : A wedge surface with variable temperature$\left(n=\frac{1+m}{2}\right)$.

Case 4 : A wedge surface with variable temperature($n=1+m$).

A positive value of n means a wall temperature which increases in flow direction. The temperature gradient of Case 4 is greater than that of Case 3 when their geometries(β) and main stream velocity(U_∞) are the same.

The boundary-value problem (7) through (9) is solved numerically for each case by using code BOUNDS. BOUNDS is a multiple shooting code[16], employing the Bulirsch-Stoer rational extrapolation algorithm[17] for solutions of initial value problems. As n increases or β approaches to zero in the region of reversed flow, it becomes more difficult to obtain converged solutions. Therefore Case 1, Case 2, Case 3, and Case 4 were calculated to $\beta=-0.004$, -0.007, -0.006, -0.025, respectively.

3. Results and Discussion

3.1. Comparison with other Results

Before presenting the detailed numerical results the validity of the present calculation procedure must be confirmed. Therefore calculated results of flow parameters are compared with those of previous studies. Table 1 and 2 display the variation of flow parameter $f''(0)$ with β. For $-0.198837<\beta<0$, there are two solutions of the governing equations, one is the type of

Table 1 Numerical values of flow parameter $f''(0)$ for accelerated and retarded flows

β	$f''(0)$		
	Present	White[21]	Evans[22]
−0.198837	0.00	0.0	0.0
−0.19	0.08588237		0.0856997
−0.10	0.31927290		
−0.05	0.40032350		0.4003225
−0.01	0.45645519		
0.00	0.46960028	0.46960	
0.30	0.77475457		
0.50	0.92768006		0.9276800
0.80	1.1202677		
1.00	1.2325877	1.23259	1.2325876

Table 2 Numerical values of flow parameter $f''(0)$ for reversed flow

β	$f''(0)$ Present	$f''(0)$ Stwartson[1]	$f''(0)$ Cebeci & Keller[3]
−0.198837	0.000		0.000 ($\beta=-0.198851$)
−0.198836	−0.001		−0.001 ($\beta=-0.198826$)
−0.194823	−0.050		
−0.183511	−0.090	−0.0970 ($\beta=-0.180$)	−0.097 ($\beta=-0.180552$)
−0.178826	−0.100		
−0.152117	−0.132	−0.1320 ($\beta=-0.15$)	−0.132 ($\beta=-0.152118$)
−0.136318	−0.140		
−0.117798	−0.143		
−0.105	−0.141714	−0.1410 ($\beta=-0.10$)	−0.141 ($\beta=-0.101763$)
−0.101	−0.140809		
−0.100	−0.140546		
−0.080	−0.132228		−0.132 ($\beta=-0.079596$)
−0.070	−0.125859		
−0.050	−0.108271	−0.1082 ($\beta=-0.05$)	−0.108 ($\beta=-0.049735$)
−0.040	−0.096637		
−0.025	−0.073658	−0.0744 ($\beta=-0.025$)	−0.0744 ($\beta=-0.024789$)
−0.010	−0.042322		
−0.009	−0.039540		−0.040 ($\beta=-0.009162$)
−0.006	−0.030292		
−0.004	−0.023039		

retarded flow($f''(0)>0$) and the other is that of reversed flow ($f''(0)<0$). But there exists a unique solution at $\beta=-0.198837$ and $\beta=0$, respectively. As can be seen in Tables 1, 2, the results of the present study are quantitatively (within the fourth decimal place) in good agreement with those of White[18] and Evans[14] in the region of accelerated and retarded flows, and those of Stewartson[3] and Cebeci & Keller[7] in the region of reversed flow.

Also the dimensionless wall shear distributions of our results coincide with Fig. 1 in reference (3). And the dimensionless velocity distributions coincide with Fig. 6. 2 in reference (14) for accelerated and retarded flows, and with Fig. 2 in reference (7) for reversed flow. The dimensionless shear $f''(\eta)$ as β is demonstrated in Fig. 2. For accelerated and retarded flows, a maximum value of the shear stress f'' moves away from the wall as β increases in the negative direction. For reversed flow, the converse is true. This maximum value increases with increasing acceleration of the flow. For retarded and reversed flows, this value occurs at about the midpoint of boundary layer and such a profile would be highly unstable. Because the shear stress near the wall has a negative value, we can see that there exists the back flow.

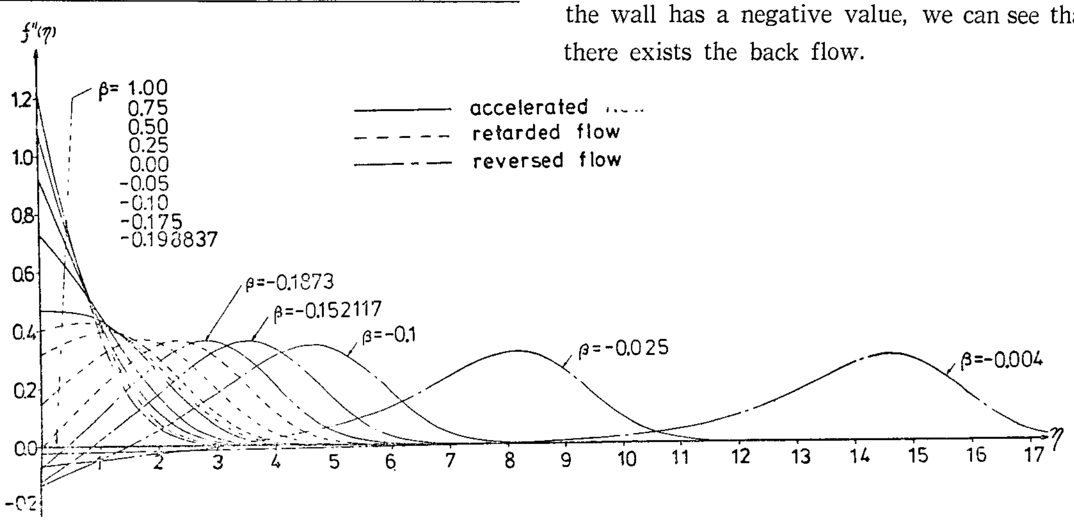

Fig. 2 The dimensionless shear f'' for accelerated, retarded and reversed flows as a function of η

3.2. Temperature Distribution

(1) Case 1 : An isothermal wedge surface ($n=0$).

The dimensionless temperature distributions in the region of accelerated and retarded flows are shown in Fig. 3. As the value of β decreases, thermal boundary layer thickness increases in the region of accelerated and retarded flows. This phenomenon occurs because thermal boundary layer thickness is inversely proportional to the square root of Reynolds number when Prandtl number is constant $\{\delta_t \propto 1/(Re \cdot Pr)^{1/2}\}$.

At the same value of β, thermal boundary

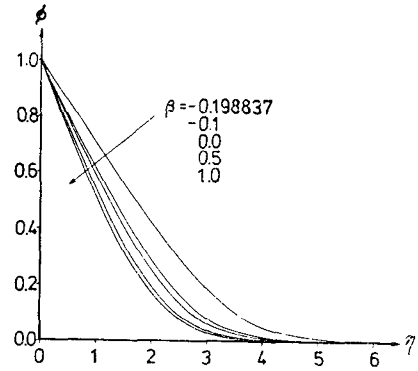

Fig. 3 The dimensionless temperature ϕ for accelerated and retarded flows as a function of η ($n=0$)

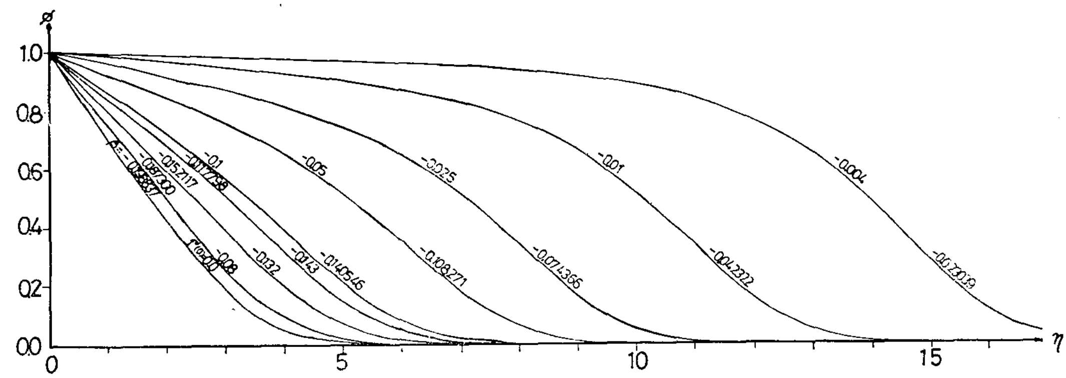

Fig. 4 The dimensionless temperature ϕ for reversed flow as a function of η ($n=0$)

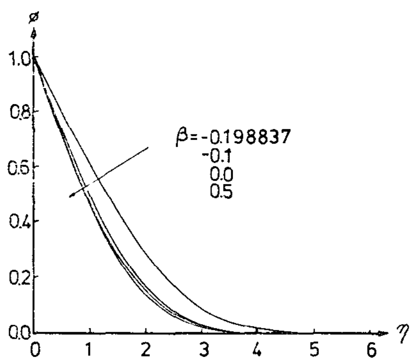

Fig. 5 The dimensionless temperature ϕ for accelerated and retarded flows as a function of η ($n=\frac{1-m}{2}$, $m\neq 1$)

layer is slightly thicker than velocity boundary layer(see Fig. 6.2. in reference [14]). The most probable explanation of the above mentioned tendency is that the ratio of the temperature and velocity boundary layer thickness is inversely proportional to the square root of Prandtl number($\delta_t/\delta \propto 1/\sqrt{Pr}$). The dimensionless temperature distributions in the region of reversed flow are plotted in Fig. 4. Back flow is induced because the momentum is not large enough to overcome the increment of pressure. As β approaches to the singular point, $\beta=0$, thermal boundary layer thickness increases due to the effect of back flow(see Fig. 1 in reference [3],

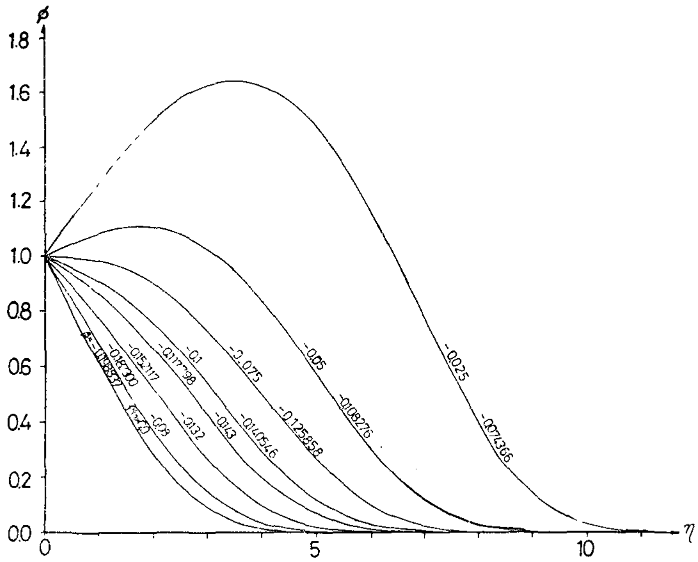

Fig. 6 The dimensionless temperature ϕ for reversed flow as a function of η $\left(n=\frac{1-m}{2},\ m\neq 1\right)$

Fig. 2 in reference [7], Fig. 2).

(2) Case 2 : A wedge surface with uniform heat flux$\left(n=\frac{1-m}{2}, m\neq 1\right)$.

Fig. 5 displays the dimensionless temperature distributions in the region of accelerated and retarded flows. For accelerated and retarded flows, as β decreases thermal boundary layer thickness increases. This trend is analoguous to that in Fig. 3. The dimensionless temperature distributions in the region of reversed flow are shown in Fig. 6. The fluid in the immediate neighborhood of the wall at any location flows from downstream to upstream region where it is in contact with a colder wall. This situation finally causes a heat flow from the fluid into the wall.

As β increases, the values of dimensionless temperature ϕ are greater than 1.0 in the region of $\beta\geq-0.075$. Because of a more vigorous heat transfer between the fluid and the wall, the thermal boundary layer of Case 1 is thicker than that of Case 2.

(3) Case 3 & Case 4 : A wedge surface with variable temperature.

For accelerated and retarded flows, the dimensionless temperature distributions of Case 3 and Case 4 are presented in Figs. 7, 8, respectively. As β decreases, thermal boundary layer thickness increases. From Fig. 7 and Fig. 8, we know that the thermal boundary layer of Case 3 is thicker than that of Case 4. This corresponds to a more vigorous heat transfer between the fluid and the solid surface. In Fig. 9 and Fig. 10, the dimensionless temperature distributions of Case 3 and Case 4 are plotted in the region of reversed flow. The value of dimensionless temperature is greater than 1.0 above $\beta=-0.072$ in Case 3. But Case 4 has the value of dimensionless temperature above 1.0 in the range of $\beta\geq-0.1$. This is also a consequence of a fluid particle heated to nearly the wall temperature being convected downstream to a place at which wall temperature is lower. Then, since the fluid particle is warmer than the wall, heat flows into the wall. Because the temperature gradient of Case 4 is greater than that of Case 3, Case 4 has the value of dimensionless temperature above 1.0 at value of β

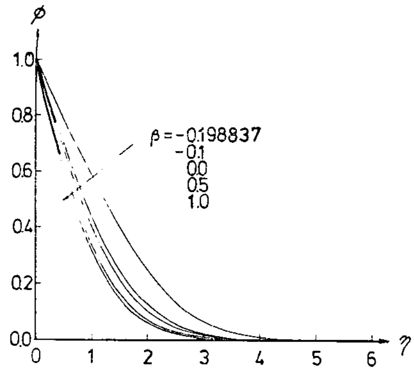

Fig. 7 The dimensionless temperature ϕ for accelerated and retarded flows as a function of $\eta\left(n=\frac{1+m}{2}\right)$

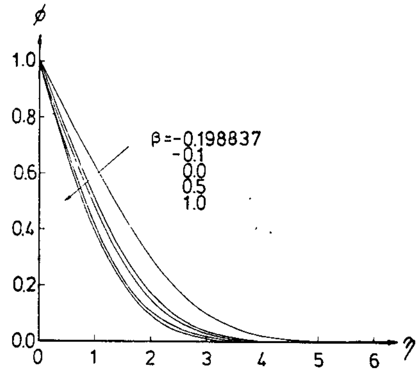

Fig. 8 The dimensionless temperature ϕ for reversed flow as a function of $\eta\left(n=\frac{1+m}{2}\right)$

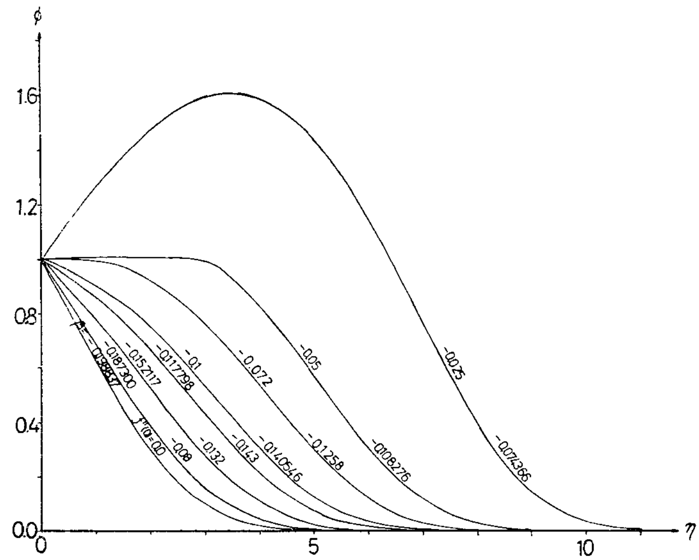

Fig. 9 The dimensionless temperature ϕ for accelerated and retarded flows as a function of η $(n=1+m)$

smaller than the value of β of Case 3.

3.3. Heat Transfer Parameter

Fig. 11 represents heat transfer parameter with various n. Because of the remarked difference of the velocity and temperature boundary layer thickness between retarded flow and reversed flow at the same value of β, there are two different values of heat transfer parameter in the region of multiple steady states. When n is zero, there are two positive values of heat transfer parameter in the range of $-0.198837<\beta\leq-0.004$. The newly found additional steady state solutions are of considerable practical interest because the heat transfar parameters for a pair of solutions(with determining physical parameters and boundary conditions) are sometimes vastly different. For example, the heat transfer rate at the isothermal wedge surface($\phi'(0)$), determined for the previously known steady

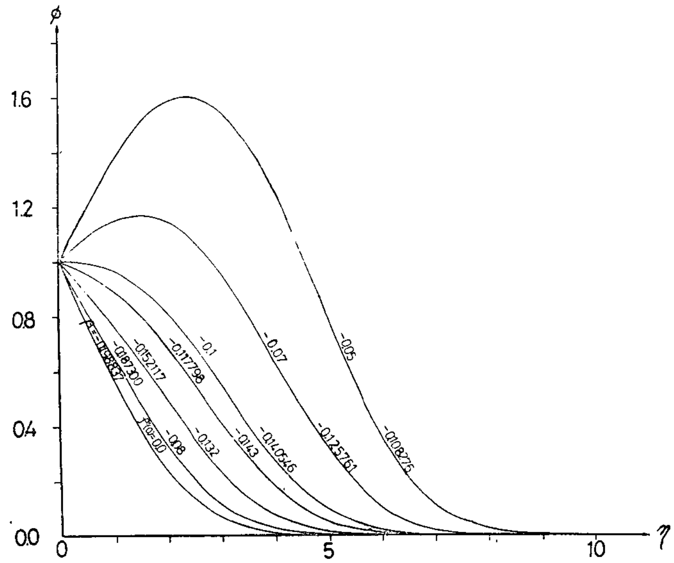

Fig. 10 The dimensionless temperature ϕ for reversed flow as a function of η ($n=1+m$)

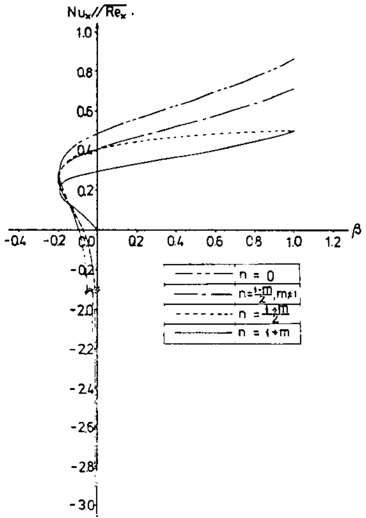

Fig. 11 Heat-transfer parameter with various n

state solution at $\beta=-0.004$, is 0.4176. That found for the second steady state solution at the same value of β is 0.0065. The ratio of these heat transfer rates is approximately 64. This striking tendency do not provide a new mechanism. They do, however, suggest that any actual flow maybe either very unstable, unsteady, or both of these. Therefore, we think that more thoughtful work will be needed to apply technological applications. Appreciable differences in heat transfer parmeter distribution are seen in Fig. 11, and the differences in Case 1 is much smaller than that in other cases. This information may be used for many purposes.

The reversal of heat flow is due to the effect of back flow, such an occurrence results in negative heat transfer coefficients(see Fig. 6). So there exists the negative value of heat transfer parameter in the range of $-0.075<\beta\leq-0.007$ when n is $\frac{1-m}{2}$ and $m\neq1$. And as shown in Fig. 11, both Case $3\left(n=\frac{1+m}{2}\right)$ and Case $4(n=1+m)$ have the negative and positive values of heat transfer parmeter in the range of $-0.072<\beta\leq-0.006$, $-0.1<\beta\leq-0.0025$, respectively (see Figs. 8, 10). We can see that the range of the negative value of heat transfer parameter coincides with the range of the dimensionless temperature above 1.0.

4. Conclusions

Theoretical analysis of forced convective heat transfer over a wedge in the region of multiple steady states has been carried out to investigate the behaviors of multiple solutions under the four cases. Multiple steady state solutions of the energy eqvation were found in the range of $-0.198837<\beta<0$.

Because momentum is not large enough to overcome the increment of pressure in the reversed flow, back flow is induced. The parameter n has quite a strong influence on the shape of the tempeɹature distributions, especially when it has large positive values. In the cases of the wedge with uniform heat flux and with variable temperature indices of $n=\frac{1+m}{2}$ and $n=1+m$, this back flow causes a heat flow from the ambient fluid into the solid surface. Such an occurence results in negative heat transfer parameter. Therefore there exist the negative and positive values of heat transfer parameter at $-0.075<\beta\leq-0.007$, $-0.072<\beta\leq-0.006$, $-0.1<\beta\leq-0.025$, respectively, in the region of multiple steady states.

An isothermal wedge, on the other hand, has two positive values of heat transfer parameter in the range of $-0.198837<\beta\leq-0.004$. Because the wedge surface is isothermal, the back flow causes a heat flow from the solid surface into the ambient fluid.

To produce such a flow exprimentally, one needs a wedge with a negative opening angle and under the conditions satisfying the above assumptions, which is much difficult to realize. Our theoretical results do not provide a new mechanism for multiple solutions. However, we think that multiple solutions occur or may occur experimentally.

References

(1) V.M. Falkner and S.W. Skan, Some Approximate Solutions of the Boundary-layer Equations, Phil Mag., Vol. 12, pp. 865~896, 1931

(2) D.R. Hartree, On an Equation Occurring in Falkner and Skan's Approximate Treatment of the Equations of Boundary Layer, Proc. Camb. Phil. Soc. 33, Part II, pp. 223~239, 1937

(3) K. Stewartson, Further Solution of the Falkner-Skan Equation, Proc. Camb. Phil. Soc. 50, pp. 454~465, 1953

(4) L.C. Burmeister, Convective Heat Transfer, Chap. 7, pp. 297~312, John Wiley & Sons, Inc., New York, 1983

(5) I. Imai, On the Heat Transfer to Constant-property Laminar Boundary Layer with Power-function Free-stream Velocity and Wall-temperature Distributions, Quart. Appl. Math., Vol. 16, pp. 33~45, 1958

(6) D. Stojanovic, Similar Temperature Boundary Layer, J. Aerospace Sci., Vol. 26, pp. 571~574, 1959

(7) T. Cebeci and H.B. Keller, Shooting and Parallel Shooting Method Solving the Falkner-Skan Boundary-layer Equation, J. of Comput. Phys., Vol. 7, pp. 289~300, 1971

(8) L. Lees & B.L. Reeves, Supersonic Separated and Reattaching Laminar Flows: I. General Theory and Application to Adiabatic Boundary-layer/Shock-wave Interactions, A.I.A.A.J. 2, pp. 1907~1920, 1964

(9) P. Orimi & B.L. Reeves, Analysis of Leading-edge Separation Bubbles on Airfoils, A.I.A.A.J. 14, pp. 1549~1555, 1976

(10) Takeo Saitoh, Natural Convection Heat Transfer from a Horizontal Ice Cylinder,

Appl. Sci. Res., Vol. 32, pp. 429~451, 1976

(11) P.J. Zandbergen and D. Dijkstra, Non-unique Solutions of the Navier-Stokes Equations for the Karman Swirling Flow, J. of Eng. Math., Vol. 11, pp. 167~188, 1977

(12) M. Lentini and H.B. Keller, Computation of Karman Swirling Flows, Lecture Notes in Comp. Sci., Vol. 76, pp. 89~100, 1978

(13) B. Gebhart, I. El-henawy, N. Kazarinoff and J.C. Mollendorf, Numerically Computed Multiple Steady States of Vertical Buoyancy Induced Flows in Cold Pure Water, J. of Fluid Mech., Vol. 122, pp. 235~250, 1982

(14) H.L. Evans, Laminar Boundary-layer Theory, Chap. 6, pp. 61~80, Addison-Wesley Pub. Co., Inc., Mass., 1968

(15) B. Gebhart, Boundary Layer Flows and Instability in Natural Convection, Adv. in Heat Transfer, Vol. 9, pp. 273~348, 1973

(16) P. Deuflhard, Nonlinear Equation Solvers in Boundary Value Problem Codes-An Invited Survey Paper, Lecture Notes in Comp. Sci., Vol. 76, pp. 40~66, 1978

(17) R. Bulirsch and J. Stoer, Numerical Treatment of Ordinary Differential Equation by Extrapolation Methods, Numerische Mathematik, Vol. 8, pp. 1~13, 1966

(18) F.M. White, Viscous Fluid Flow, Chap. 4, pp. 273~284, McGraw-Hill, Inc., New York, 1974